Proceedings of the 8th European Symposium on Corrosion Inhibitors (8 SEIC)
Ann. Univ. Ferrara, N.S., Sez. V, Suppl. N. 10, 1995.

TESTING OF INHIBITORS FOR CO_2 CORROSION USING THE ELECTROCHEMICAL TECHNIQUES

S.NESIC*, W. WILHELMSEN*, S. SKJERVE** AND S.M. HESJEVIK**
* Institute for Energy Technology - Kjeller (Norway)
** Statoil - Trondheim (Norway)

ABSTRACT

Tests have been carried out in the laboratory to study two different CO_2 corrosion inhibitors; one amine based inhibitor (ABI) and one imidazoline based inhibitor (IBI) using a variety of electrochemical techniques. Both inhibitors are considered for application in the North Sea for reducing the CO_2 corrosion problems in the pipelines carrying oil and gas.

It was found in glass cell experiments that the temperature and pH had a negligible effect on the performance of both inhibitors. The presence of NaCl degraded the performance of the ABI but did not affect protectiveness obtained with the IBI. A condensate oil did not interfere with performance of the inhibitors. However, a crude oil degraded the performance of the ABI significantly. It was found that the IBI corrosion inhibitor was incompatible with a phosphinocarboxylic acid based scale inhibitor. The performance of IBI was very poor in the presence of the surface films. Finally, the mechanism of protection for both inhibitors was explained with a model including a Frumkin-type adsorption isotherm and a surface blockage effect.

INTRODUCTION

The effectiveness of a CO_2 corrosion inhibitor is dependent upon its composition and the conditions under which it is applied. Some of the most important field parameters are: temperature, pressure, presence of different fluid phases in the pipeline and their concentration (gas/liquid ratio, brine/hydrocarbon ratio), flow regime and emulsion properties. Further, the presence of corrosion films at the metal surface, inhibitor composition, acidity, solubility and dispersibility, inhibitor film forming characteristic and inhibitor compatibility with other chemicals are very important.[1] Testing of inhibitors intended for field application in a laboratory is difficult because of the complexity of the inhibition mechanism and the large number of factors that affect it. There is no universal test method on laboratory scale for testing of CO_2 corrosion inhibitors. Several different tests have to be carried out in order to study parameters which may affect inhibitor performance in the field applications.

Electrochemical techniques are often used to study inhibitor performance in laboratory tests. Selection of the type of electrochemical techniques for inhibitor evaluations depends on the objectives of the study. Dawson et al.[2] have investigated various electrochemical techniques in laboratory studies: potentiodynamic sweep, polarisation resistance, electrochemical impedance, galvanic systems and electrochemical noise. They have suggested application of a full range of different techniques to identify the parameters of interest and then focused on the most appropriate method(s) for the particular application.

In the present study tests have been carried out in the laboratory to study two different CO_2 corrosion inhibitors; one amine based inhibitor (ABI) and one imidazoline based inhibitor (IBI) using a variety of electrochemical techniques. Both inhibitors are considered for application in the North Sea for reducing the CO_2 corrosion problems in the pipelines carrying oil and gas. The two inhibitors were tested jointly at the Institute for Energy Technology (IFE) and Statoil.

In the following text the test apparatus and procedures are described, followed by the presentation of the results on the effects of inhibitor concentration, temperature, pH, NaCl, precorrosion, partitioning and compatibility with a scale inhibitor. At the end

a simple mechanistic model is presented which can account for the effect of the inhibitors on the corrosion rate.

EXPERIMENTAL

Equipment

Most of the experiments presented below were conducted at IFE in glass cells. The precorrosion, compatibility and partitioning experiments were conducted at Statoil in glass cell and autoclave experiments. The description of different experimental set-up follows.

Glass cells experiments. Experiments were conducted at atmospheric pressure in a battery of eight glass cells. All components of the cells were made form borosilicate glass or PTFE. Gas (CO_2) was continuously bubbled through the cells. The corrosion process was studied with electrochemical techniques. A three electrode set-up (Figure 1) was used in all electrochemical experiments. A rotating cylinder electrode with a speed control unit (0-5000 *rpm*) was used as the working electrode. The specimen was machined from the parent material into a cylinder 10 mm in diameter and 10 mm long. The exposed area of the specimen was 3.14 cm^2. A concentric platinum ring was used as a counter electrode. A saturated Ag/AgCl reference electrode was used externally, connected to the cell via a Luggin capillary and a porous wooden plug. The speed of rotation of the working electrode was controlled with the aid of a stroboscope. The pH was followed with an electrode directly immersed into the electrolyte. Temperature was followed with a Pt-100 probe which also served as an input for the temperature regulating system - a hot plate combined with a magnetic stirrer. The concentration of Fe^{++} in the electrolyte was measured occasionally using a spectrophotometric method. The concentration of CO_2 in the electrolyte was also measured in selected experiments. Prior to immersion the carbon steel specimen surfaces were polished with 500 and 1000 grit SiC paper, degreased with acetone and finally rinsed with alcohol.

Partitioning experiments. The partitioning experiments were conducted in somewhat different glass cell equipment (Figure 2). Equal amounts of water (with 1% NaCl, initial pH-value adjusted to 4.0) and refined condensate oil were placed into a glass container and purged with CO_2 gas for about three hours. In the first experi-

ment the "oil-conditioned" water was pumped from the bottom of the container into the glass cell equipped for corrosion measurements. In another similar experiment, the inhibitor was first added to the conditioning container and only after one hour the inhibited water phase was pumped from the bottom of the container into the glass cell.

Precorrosion experiments. The effect of precorrosion on the inhibitor efficiency was studied in autoclaves. In order to remove oxygen, the electrolyte was purged with CO_2 typically overnight and then transferred into the autoclave. In all experiments carried out in autoclaves the partial pressure of CO_2 (pco_2) was 2.0 *bar*. The initial pH in the solution was adjusted to 4 and freely increased as the corrosion process proceeded. The precorrosion process was conducted in the autoclave itself. After one week of precorrosion the electrolyte was replaced by a fresh one and the inhibitor was added.

A three electrode system was used for polarisation resistance measurements including a platinum counter electrode and a saturated calomel reference electrode connected to the cell via a salt bridge. Three working electrodes were used: one for polarisation resistance measurements and another two for AC impedance measurements (two-electrode set-up).

Water chemistry

Water chemistry is one of the most important factors affecting the corrosion rate so significant attention has been given to this matter. In all the experiments conducted water preparation included: water purification by distillation or reverse osmosis and bubbling with CO_2. The same electrolyte: distilled water + 1 mass% NaCl was used in all experiments. Continuous CO_2 bubbling was maintained throughout all experiments. From previous measurements it is known that the O_2 content in the glass cells under continuous CO_2 bubbling is below 20 *ppb*. Occasionally addition of HCl and $NaHCO_3$ has been used in all experiments to achieve the desired pH.

Material

In all experiments a low carbon X65 steel was tested which is a typical pipeline steel. Chemical composition of the steel is given in Table 1.

Table 1. Chemical composition of the X65 steel used for the working electrode (mass%)

C	Mn	Si	P	S	Cr	Cu	Ni	Mo	Al	V	Sn	Ti	Nb
0.064	1.54	0.25	0.013	0.001	0.05	0.04	0.04	0.007	0.041	0.035	0.002	0.002	0.041

Corrosion measurements

The corrosion process was monitored in-situ with several electrochemical techniques: polarisation resistance, AC impedance and potentiodynamic sweep. A three-electrode set-up was used in most of the electrochemical experiments. In addition in some experiments two-electrode AC impedance measurements were used for in-situ corrosion monitoring.

The polarisation resistance measurements were conducted by polarising the working electrode 5-10 mV around the free corrosion potential and scanning at 0.1 mV/s. The solution resistance was measured independently using AC impedance and subtracted from the polarisation resistance. The AC impedance measurements were done by applying an oscillating potential to the working electrode 5-10 mV_{rms} around the free corrosion potential using the frequency range typically 10 mHz - 10 kHz. At the end of each experiment the potentiodynamic sweeps were conducted, starting at the corrosion potential and sweeping typically 600 mV below and 150 mV over the free corrosion potential. Some experiments were repeated by sweeping in the opposite direction without a significant difference in the results. Typical scanning rate used was 0.1 - 0.3 mV/s.

Electrochemical measurements were made with a Gamry Instruments Inc. potentiostat including an eight channel multiplexer and a Solartron 1286 potentiostat with a Solartron 1255 EIS analyser and a multiplexer.

RESULTS AND DISCUSSION

Inhibitor concentration effect

The effect of inhibitor concentration on the corrosion rate and potential is shown in Figure 3 (ABI) and Figure 4 (IBI). In this and all other glass cell and glass loop experiments the inhibitor was added a few hours after the corrosion process started when a stable corrosion rate was obtained. For ABI one can notice in Figure 3 that after introducing the inhibitor, the corrosion rate decreased sharply and then stabilised typically within 1 - 2 hours. For the IBI the corrosion rate also decreased sharply (Figure 4), however a longer time was required before a steady state was achieved. Addition of the inhibitor also caused a rapid increase in the corrosion potential for both inhibitors.

The steady state corrosion rate and inhibitor efficiency vs. inhibitor concentration are shown in Figure 5a (ABI) and Figure 5b (IBI). It can be seen that the corrosion rate is reduced over 90% when 20 ppm of ABI or IBI is added. Further addition of the inhibitor in both cases produces a much smaller effect. The linearity of the corrosion rate (CR) vs. inhibitor concentration (C_{inh}) data seen for both inhibitors suggests a power law type of dependence as a first approximation:

$$CR = \mathrm{A} \cdot \left(c_{inh}\right)^{n} \tag{1}$$

where A is a constant. When such a function is fitted to the experimental data it is found that for the ABI: A=1 and n=-0.8 while for the IBI: A=1.3 and n=-1. This kind of a relationship is determined in a limited range of inhibitor concentrations and any extrapolations are uncertain. It can be noticed that the fit of the straight line is not so good at lower concentrations especially for the IBI what will be discussed later.

In Figure 6 where potentiodynamic sweeps are presented for different inhibitor concentrations one can begin to deduce the mechanism of the protection. As a first rough approximation one can say that both inhibitors act similarly by slowing down the cathodic and the anodic reactions. However the effect on the anodic reaction is much stronger. The cathodic reaction is inhibited by a factor of 2-3 when the inhibitor concentration is increased from 0 to 200 ppm. At the same time the anodic reaction is slowed down approximately two orders of magnitude.

If the corrosion potential is plotted against the corrosion current (measured at different points in time), a so called "pseudo-polarisation" plot is obtained [3] (Figure 7). This *trajectory* of the "corrosion point" obtained after the addition of 20 ppm of the inhibitor is in Figure 7 overlaid with the steady state potentiodynamic sweeps measured with and without the presence of inhibitor.

For the ABI inhibitor (Figure 7a) one can notice that the anodic reaction is inhibited very rapidly within the first 15 min leading to a rapid increase in the corrosion potential and to a drop in the corrosion current seen in Figure 3. The cathodic reaction remains nearly constant in this short period. Subsequently, the anodic reaction remains practically unchanged while the cathodic reaction is gradually inhibited. This is seen in Figure 3 as a gradual decrease of both the corrosion current and the corrosion potential towards the steady state. It is still difficult to propose an explanation for this observation. However it can be speculated that the ABI molecules are initially attracted towards the anodic sites (e.g. imperfections on the metal surface) leading to a significant decrease in the iron dissolution rate, without affecting the cathodic reaction directly. Subsequently due to the lateral interactions between the adsorbed inhibitor chains, the transport of the cathodic species is hindered leading to a decrease in the cathodic reaction.

For the IBI inhibitor (Figure 7b) one can notice similar behaviour as observed for the ABI but only within the first measuring point: rapid inhibition of the anodic reaction. However, in case of the IBI after the initial 15 min. both reactions are further inhibited leading to a nearly horizontal line in Figure 7b. It takes quite a long time (nearly two days under stagnant conditions) before a steady state is achieved.

The SEM images of the cross section of the metal surface for different IBI concentration are shown in Figure 8. At 2 *ppm* of IBI where no significant corrosion protection was obtained (efficiency <10%) the surface of the metal looks similar to the one often seen without an inhibitor present. At 20 *ppm* what is close to an optimal inhibitor concentration (efficiency 96%), the surface looks smooth and evenly corroded. However, at 200 *ppm* what is an excessively high concentration of the inhibitor (efficiency >99%) a pit-like corrosion attack can be observed. The average pit depth corresponds to a 2 *mm/y* attack what is higher than the uninhibited corrosion rate at the same conditions.

Temperature effect

Temperature (t) can affect the adsorption of inhibitor to the metal surface. If the inhibitor is adsorbed due to chemisorption, an increase in temperature can result in increased inhibitor efficiency. A physical adsorption will not be affected by the temperature.[4]

The efficiency of the inhibitors at three different temperatures tested is shown in Table 2 for 20 ppm of the inhibitor at pH 4 and stagnant conditions. One can say that no practically significant difference in the performance of the inhibitor can be noticed with temperature for either of the inhibitors. The small differences are of the same order of magnitude as the experimental error.

Table 2. Efficiency of the inhibitors at different temperatures, c_{inh}=20 ppm, pH 4, stagnant conditions.

	20°C	50°C	80°C
ABI efficiency	93±1 %	96±1 %	93±1 %
IBI efficiency	96±1 %	97±1 %	98±1 %

pH effect

Schmitt et al.[5] reported that the inhibitor efficiency was reduced with decreasing pH. In the present study it was found that the pH did not have a strong effect on the performance of the inhibitors tested. The inhibitors efficiency is presented in Table 3 for 20 *ppm* of inhibitor at t=20°C, p_{CO_2}=1 *bar* and stagnant conditions. The spreading of the results fall within the margin of experimental error.

Table 3. Efficiency of the inhibitors at different pH, c_{inh}=20 ppm, t=20°C, p_{CO_2}=1 bar, stagnant conditions.

	pH 4	pH 5	pH 6
ABI efficiency	93 ±1 %	89 ±1 %	93 ±1 %
IBI efficiency	96±1 %	96±1 %	97±1 %

NaCl effect

Tests were conducted to study the effect of NaCl concentration on the performance of the two inhibitors. The effect of NaCl concentration on the performance of ABI was significant. The efficiency of the inhibitor was reduced from 94% at 1 mass% NaCl concentration to 84% with 10 mass% NaCl present (Figure 9). It is possible that the Cl^- ions (which are a weak inhibitor) competed with the ABI molecules for adsorption on the metal surface. However the presence of NaCl had no consistent effect on the performance of the IBI.

Partitioning effect

Effect of condensate. Equal amounts of water (1% NaCl with pH-value adjusted to 4.0) and refined condensate were placed into a container and purged with CO_2. The water phase in the bottom of the container was then pumped into a glass cell equipped for electrochemical experiments. For the inhibitor experiments, injection of the inhibitor on top of the condensate phase was carried out 1 hour before transferring the electrolyte. The corrosion measurements are shown in Figure 10. The corrosion rate without inhibitor stabilised around 1 *mm/y* which is similar to the measurements obtained in non-conditioned electrolyte. The stabilised corrosion rates with the inhibitor present are somewhat lower than earlier observed in unconditioned water. However, the effect of condensate is not significant and falls within the margin of experimental error.

Effect of crude oil. In one experiment the presence of a crude oil phase laying on top of the water phase was investigated (Figure 11). It was found that there was no effect of the crude oil on the base-line corrosion rate (without the inhibitor). However, with

the oil present the efficiency of 20 *ppm* of ABI inhibitor was reduced from 93% (measured without oil) to approximately 80%. It is possible that part of the inhibitor was consumed by the oil-water interface. This is supported with the visual observation that the ABI strongly affected the tendency towards emulsification of the oil/water mixture.

Compatibility study

In one set of autoclave experiments conducted at 50°C , 2 bar CO_2 pressure and pH 4, the compatibility of the IBI corrosion inhibitor and a typical scale inhibitor (phosphinocarboxylic acid based) was tested. First it was observed that the scale inhibitor does not in itself affect the corrosion rate. When 30 ppm of IBI was subsequently added it had no effect on the corrosion rate (Figure 12). The same ineffectiveness of the IBI was observed when the two inhibitors were added simultaneously. However, when the IBI was added first, subsequent addition of the scale inhibitor did not change the obtained inhibition.

These results suggest that the incompatibility of the two chemicals stems from the competition for adsorption to the metal surface. It seems that IBI was unable to displace the scale inhibitor once it was adsorbed on the surface. However the opposite seems to be true as well. This stresses the high sensitivity of the IBI to the state of the metal surface. In addition, the incompatibility between scale and corrosion inhibitor when they are added simultaneously may be a direct result of the general anionic and cationic natures of the scale and corrosion inhibitors respectively. Corrosion inhibitor and scale inhibitor compatibility has also been studied by Lawless et al.[6] They found that an imidazoline based corrosion inhibitor and a polyphosphinocarboxylic acid based scale inhibitor are an incompatible blend.

Precorrosion effect

In general most of the laboratory work concerning the inhibitor performance has been focused on freshly prepared metal surfaces. However, Våland 7 found that some corrosion inhibitors were not active when corrosion films were present at the metal surface. Other inhibitors were able to modify the film when added to the solution before the film formation started. Kapusta et al. 8 have also found that inhibitor performance was strongly affected by the condition of the metal surface.

The performance of the IBI on a surface with a protective film is shown in Figure 13. The experiment began by introducing the specimen into the autoclave where 2 bar CO_2 pressure, and 80°C were maintained. The corrosion proceeded at a high rate for 24 hours (3-10 *mm/y*). Due to the rapid release of the corrosion products into the electrolyte, the Fe^{2+} concentration increased towards and probably beyond the saturation point followed by the corresponding pH increase. At 80°C the precipitation process proceeds fast which leads to formation of a protective iron carbonate film. This process started approximately 24 hours after initiation of the experiment and can be seen on Figure 13 as a gradual decrease of the corrosion rate which within one week was reduced to a stable value of approx. 0.5 *mm/y*. The electrolyte was then substituted with a fresh one (pH 4) and 30 ppm of IBI was added short after. Two opposing processes occurred simultaneously. Due to the sudden decrease in pH the protective film began to dissolve which normally leads to an increase in the corrosion rate. On the other hand the inhibitor was supposed to decrease the corrosion rate. It seems that the former effect dominated and the inhibitor had very little effect as the corrosion rate increased to nearly 1 *mm/y* and stabilised there. A further addition of the inhibitor (c_{total}=60 *ppm*) decreased the corrosion rate to around 0.2 *mm/y* which is nearly an order of magnitude higher than measured previously on clean surfaces. After the total of 12 days the experiment was terminated.

The AC impedance measurements from the same experiment are shown in Figure 14. The initial semicircle indicating activation controlled corrosion was transformed as the experiment proceeded indicating the presence of a mass transfer barrier - probably a surface film. The SEM image of the cross section of the specimen surface is shown in Figure 15. The structure of the surface films confirms the previous explanation. A thin porous film (probably iron carbide), which was formed within the first 24 hours of the experiment when the corrosion proceeded very fast, is found adjacent to the metal surface. On top of the carbide layer, dense crystals were found, most probably composed of iron carbonate which precipitated subsequently. The relatively open structure of the carbonate film testifies of the dissolving process which occurred when the electrolyte was changed. Very poor performance of the IBI was obtained in a similar experiment conducted on a specimen precorroded in a separate cell and subsequently transferred to the autoclave at 50°C. That specimen had a good protective film to begin with which was then dissolved in the autoclave. The inhibitor was completely unable to protect the metal surface under such conditions.

MECHANISTIC MODEL

One of the simplest ways to account for the inhibition of a charge transfer reaction at a metal surface is to assume a linear relationship between the rate of the reaction (i_{cor}) and the degree of surface coverage with the inhibitor (θ): [10, 11]

$$(i_{cor})_\theta = (1-\theta)(i_{cor})_{\theta=0} + \theta(i_{cor})_{\theta=1} \tag{2}$$

Assuming that $(1-\theta)(i_{cor})_{\theta=0} >> \theta(i_{cor})_{\theta=1}$ equation (2) describes a pure blockage effect by the inhibitor: the degree of protection is proportional to the coverage of the electrode surface:

$$\frac{(i_{cor})_\theta}{(i_{cor})_{\theta=0}} = 1-\theta \tag{3}$$

From these assumptions it follows that the inhibitor efficiency:

$$\eta = \left(1 - \frac{(i_{cor})_\theta}{(i_{cor})_{\theta=0}}\right) \times 100\% = \theta \times 100\% \tag{4}$$

is equivalent to the surface coverage expressed in percents. By using the equation (3) the relationship between the inhibitor concentration (c_{inh}) and the surface coverage (θ) can be plotted for the present inhibitors as shown in Figure 16. Different adsorption isotherms were tried for explanation of the obtained data (Langmuir-, Temkin- and Frumkin-type). Only the Frumkin isotherm:

$$K_{a/d}\, c_{inh} = \left(\frac{\theta}{1-\theta}\right) e^{-f\theta} \tag{5}$$

was successful in reproducing the character of the measured curve for both inhibitors. Similar was found by Dawson et al.[2] who studied performance of a model inhibitor. The best-fit values of the equilibrium constant for the adsorption/desorption process ($K_{a/d}$) and the attraction constant (f) characterising the interaction of adsorbed inhibitor species with each other, are given in Table 4.

Table 4. Best-fit values of the parameters in the Frumkin isotherm for the two inhibitors

	$K_{a/d}$	f
ABI	140000	1.3
IBI	40000	4

These values are of the similar order of magnitude as found by Dawson et al.[2] It is now interesting to see how does this simple analysis correspond to the findings shown previously (Figure 5). The power law relationship (1) was deduced between the inhibitor concentration (c_{inh}) and the corrosion rate. By assuming that the coverage is very high ($\theta \approx 1$), the Frumkin equation (5) is reduced to:

$$1-\theta = \frac{e^{-f}}{K_{a/d}c_{inh}} \tag{6}$$

Substituting $1-\theta$ from equation (3) gives:

$$i_{cor} = (i_{cor})_{\theta=0}\frac{e^{-f}}{K_{a/d}c_{inh}} \tag{7}$$

It can be seen that the exponent on (c_{inh}) is now theoretically derived to be n=-1 for higher inhibitor concentrations. This agrees well with the best-fit value for the IBI (Figure 5b) and is somewhat higher than the n=-0.8 obtained for the ABI (Figure 5a). Taking into account that the power-law relationship cannot be theoretically derived for lower inhibitor concentrations the agreement can be considered as good. It can be concluded that for predicting purposes one can use the previously shown model including a Frumkin-type adsorption isotherm and a surface blockage effect. Substitution of the surface coverage (θ) in the Frumkin isotherm by efficiency (η) gives us the desired relationship between the inhibitor concentration and the inhibitor efficiency (η):

$$K_{a/d}c_{inh} = \left(\frac{\eta}{100-\eta}\right)e^{-\frac{f\eta}{100}} \tag{8}$$

Using the previously defined constants for $K_{a/d}$ and f from Table 4 and by solving equation (8) one can calculate the inhibitor efficiency given the inhibitor concentration. Comparison of this model and the experimental data for the two inhibitors is shown in Figure 17. For the IBI inhibitor the model is able to capture the sudden transition from low to high inhibitor efficiency in the region $2\ ppm < c_{inh} < 6\ ppm$.

CONCLUSIONS

- It was found in glass cell experiments that the corrosion rate was reduced over 90% when 20 ppm of the amine based inhibitor (ABI) or the imidazoline based inhibitor (IBI) were added.
- The temperature and pH had a negligible effect on the performance of both inhibitors.
- The presence of NaCl degraded the performance of ABI but did not affect protectiveness obtained with IBI.
- There was no effect of a light condensate or a crude oil on the base-line corrosion rate without the inhibitors present. Furthermore, the condensate did not interfere with performance of the inhibitors. However, the crude oil degraded the performance of the ABI.
- The IBI corrosion inhibitor was incompatible with a phosphinocarboxylic acid based scale inhibitor. The incompatibility of the two chemicals probably stems from the competition for adsorption to the metal surface.
- The performance of IBI was very poor in the presence of surface films (protective or unprotective). In general the inhibitors seemed very sensitive to the state of the metal surface prior to adsorption. It is likely that the changes of the metal surface due to the precorrosion process were responsible for weaker performance of the inhibitor rather than the film itself as a diffusion barrier.
- The mechanism of protection for both inhibitors can be explained and predicted with a model including a Frumkin-type adsorption isotherm and a surface blockage effect.

REFERENCES

1. Y. WU, "Corrosion Inhibitor screening tests and selection for field applications", Corrosion/94, paper no. 43, (Houston, TX: NACE International, USA, 1994).
2. J. L. DAWSON, A. N. ROTHWELL, T. G. WALSH, K. LAWSON, J.W. PALMER, "Electrochemical measurements for inhibitor assessments", Corrosion/93, paper no. 108, (Houston, TX: NACE International, USA, 1993).
3. J. L. CROLET, S. OLSEN, W. WILHELMSEN, "Influence of a Layer of Undissolved Cementite on the Rate of the CO_2 Corrosion of Carbon Steel", Corrosion/94, paper no. 4, (Houston, TX: NACE International, USA, 1994).
4. G. TRABANELLI, "Fundamental and general aspects of inhibition science, Corrosion/89, paper no. 133, (Houston, TX: NACE International, USA, 1989).
5. G. SCHMITT, M. KRIECK-DEFRAIN, "pH-Static Experiments in High Pressure CO_2 Corrosion of Steel, Effect on Scale Morphology and Chemical Composition, Corrosion rate, Pitting Susceptibility and Inhibitor Performance", Laboratory for Corrosion Protection, Iserlohn Polytechnic, Frauenstuhlweg 31, D-5860 Iserlohn, Germany, 1990.
6. T. A. LAWLESS, H. M. BOURNE, J.R. BOLTON, "Examining the potential for corrosion inhibitor and scale inhibitor compatibility in a multifunctional squeeze strategy", SPE 25167, SPE International Symposium on Oilfield Chemistry, New Orleans 1993.
7. T. VÅLAND, "CO_2 corrosion inhibitors", in Oil Field Chemicals, Norwegian Society of Chartered Engineers, Geilo, Norway 1992.
8. S. D. KAPUSTA, P. R. RHODES, S.A. SILVERMAN, "Inhibitor testing procedures for CO2 environments", Corrosion/91, paper no. 471, (Houston, TX: NACE International, 1991).
9. S. NESIC, G. SOLVI, AND J. ENERHAUG, "Comparison of the Rotating Cylinder and Pipe Flow Tests for Flow Sensitive CO_2 Corrosion", Corrosion/95, paper no. 130, (Houston, TX: NACE International, 1995).
10. J. LIPKOWSKI, Z. GALUS, "On the Present Understanding of the Nature of Inhibition of Electrode Reactions by Adsorbed Neutral Organic Molecules", Electroanalytical Chemistry and Interfacial Electrochemistry, 61 (1975) 11-32.

11. R. PARSONS, "The Effect of Specific Adsorption on the Rate of an Electrode Process", Electroanalytical Chemistry and Interfacial Electrochemistry, 21 (1969) 35-43.

12. M.V. POSPELOV, A.V. IGNATOV, V.V. YAMINSKY, A.V. FOKIN, "Hydrophobic Interaction in Inhibiting Acid Corrosion of Steel by Aliphatic Amines", 6th European Symposium on Corrosion Inhibitors Ann. Univ. Ferrara, N.S., Sez.V, Suppl.N.8, 1985.

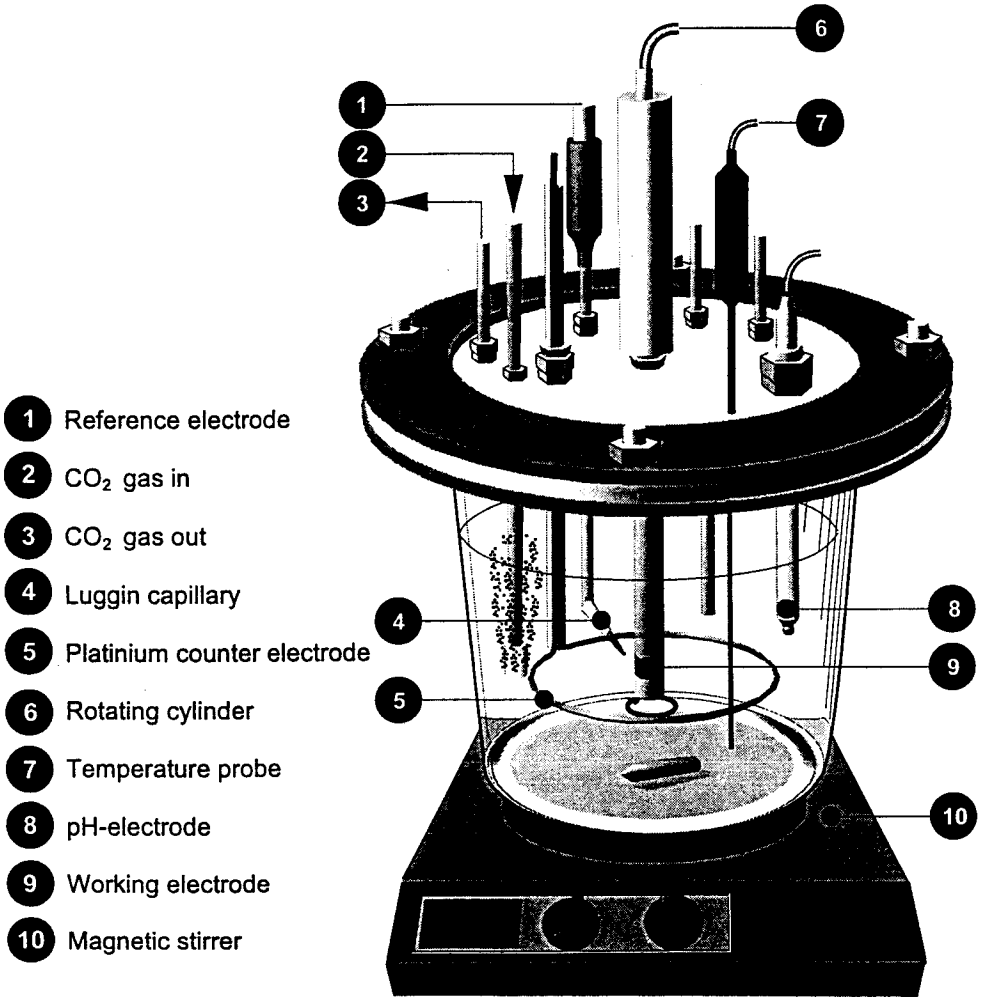

Figure 1. Schematic of the glass cell.

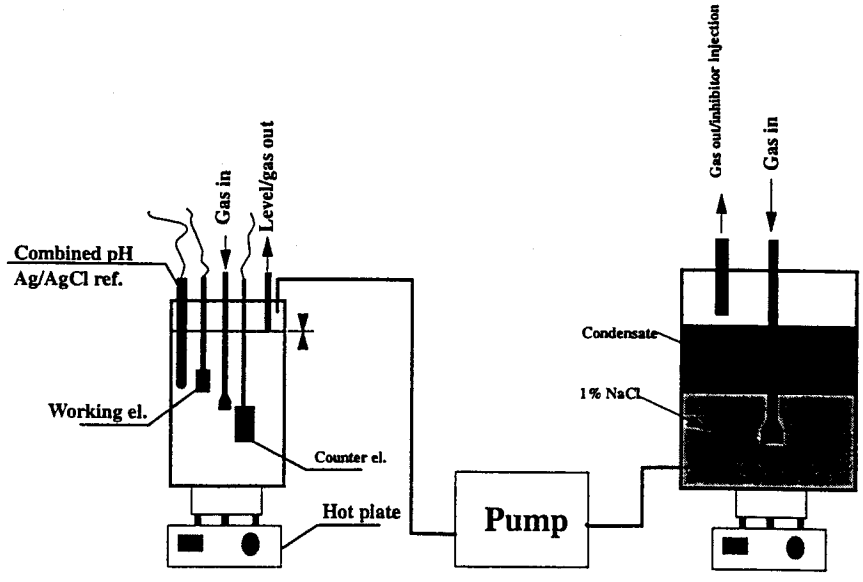

Figure 2. Schematic of the glass cells used in the inhibitor partitioning experiments.

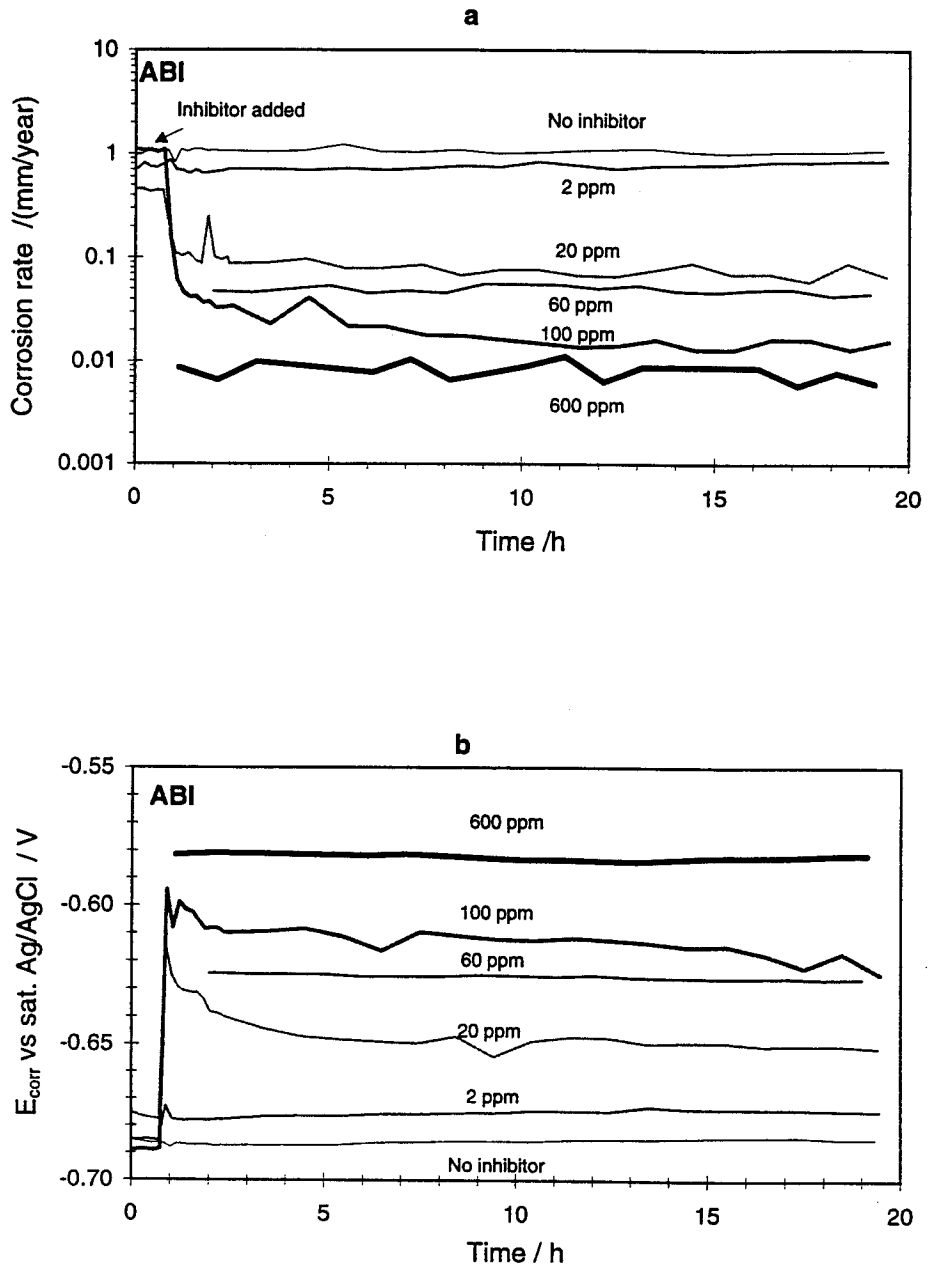

Figure 3. The effect of amine based inhibitor concentration on the (a) corrosion rate, (b) corrosion potential; pH 4, t=20°C, pco_2=1 bar, stagnant.

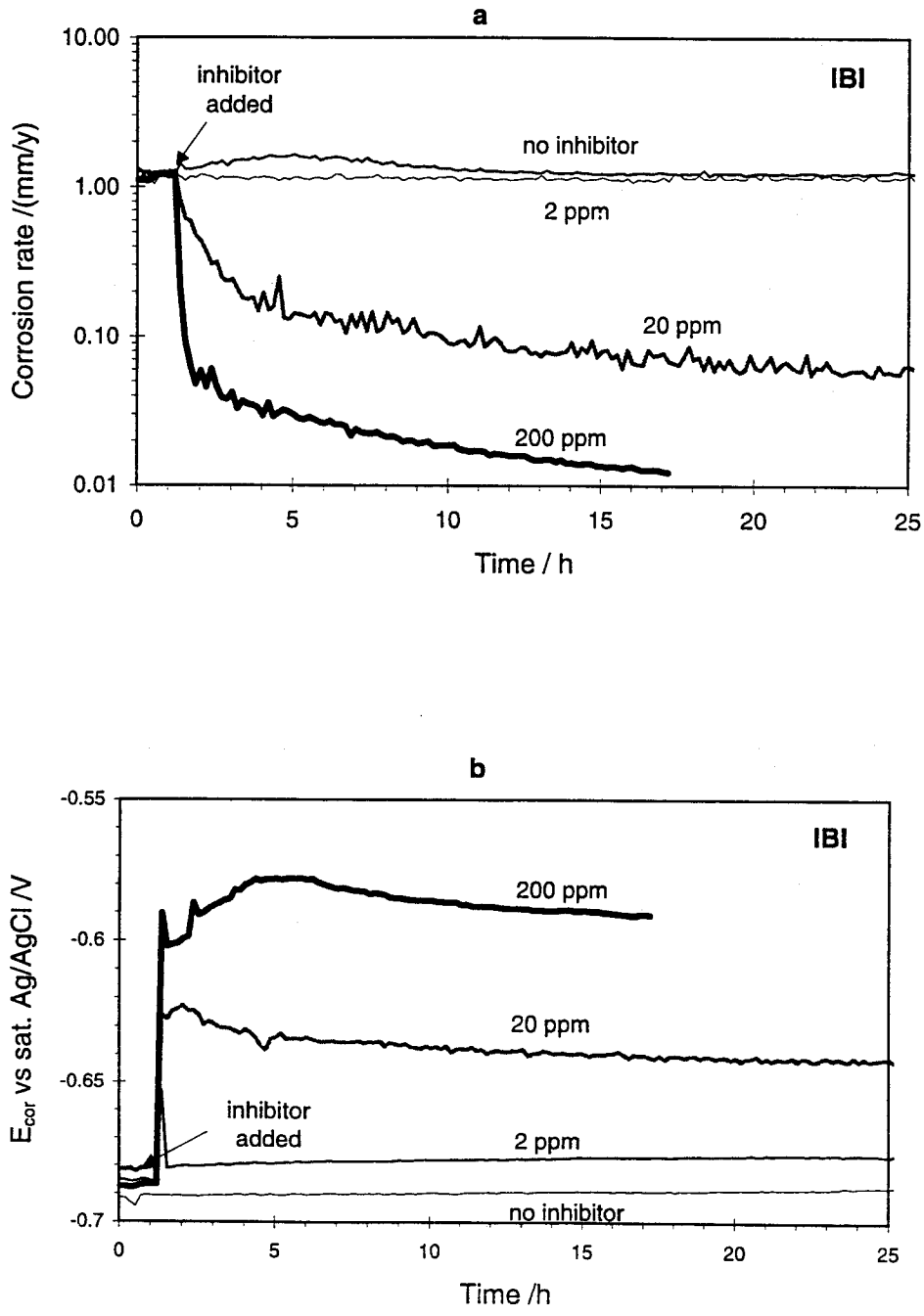

Figure 4. The effect of imidazoline based inhibitor concentration on the (a) corrosion rate, (b) corrosion potential; pH 4, t=20°C, pco_2=1 bar, stagnant.

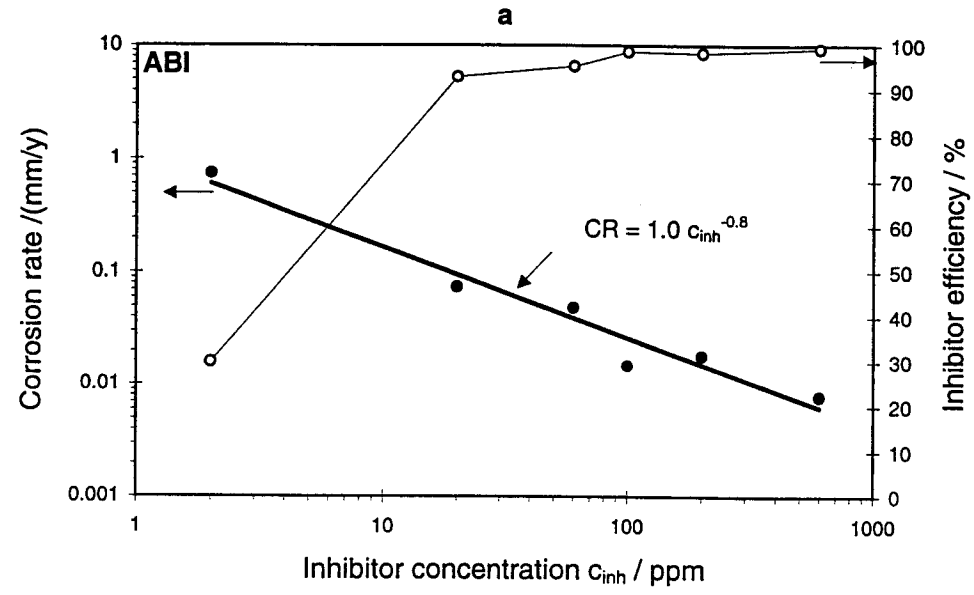

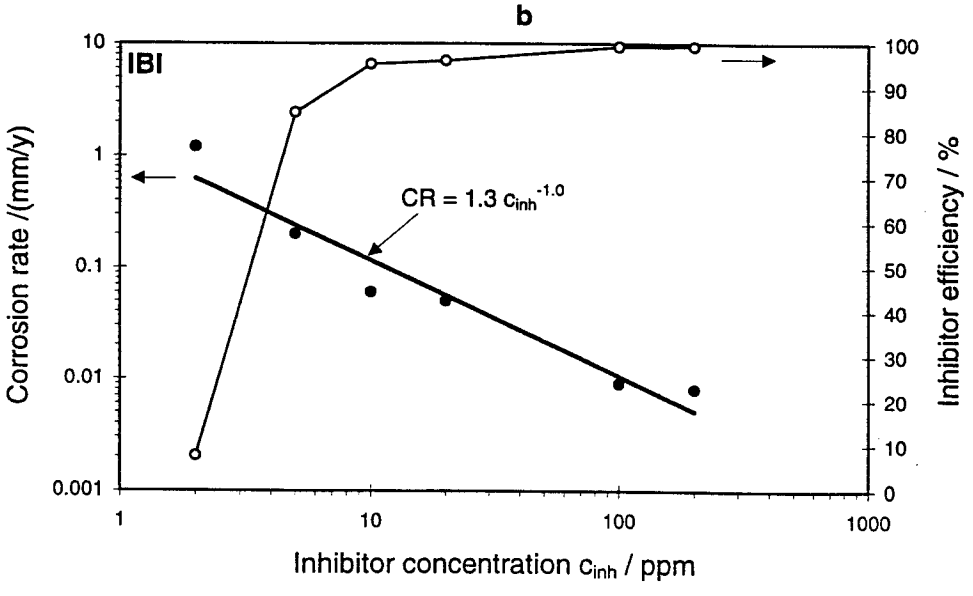

Figure 5. Inhibitor efficiency vs. concentration; pH 4, t=20°C, p_{CO_2}=1 bar, stagnant; a) amine based inhibitor (ABI), b) imidazoline based inhibitor (IBI).

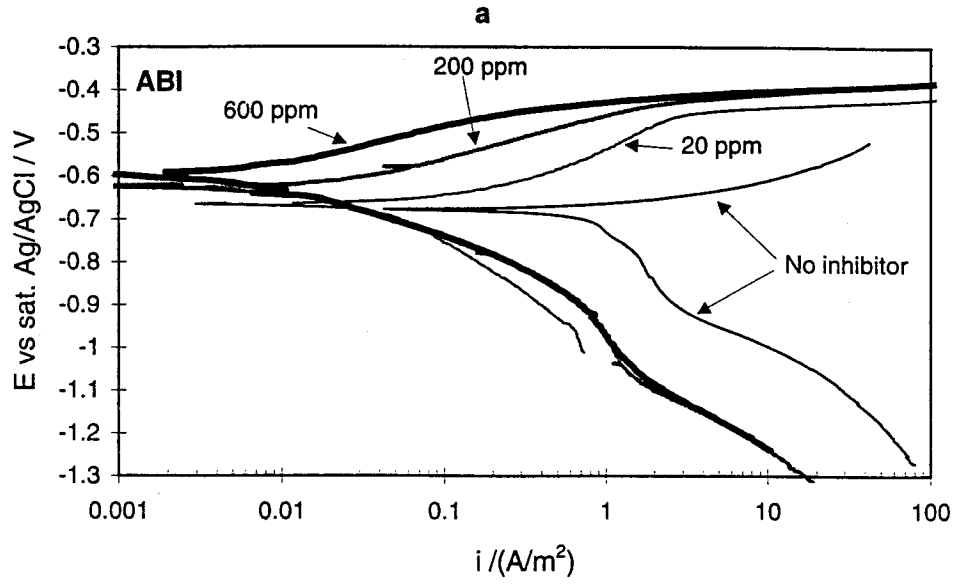

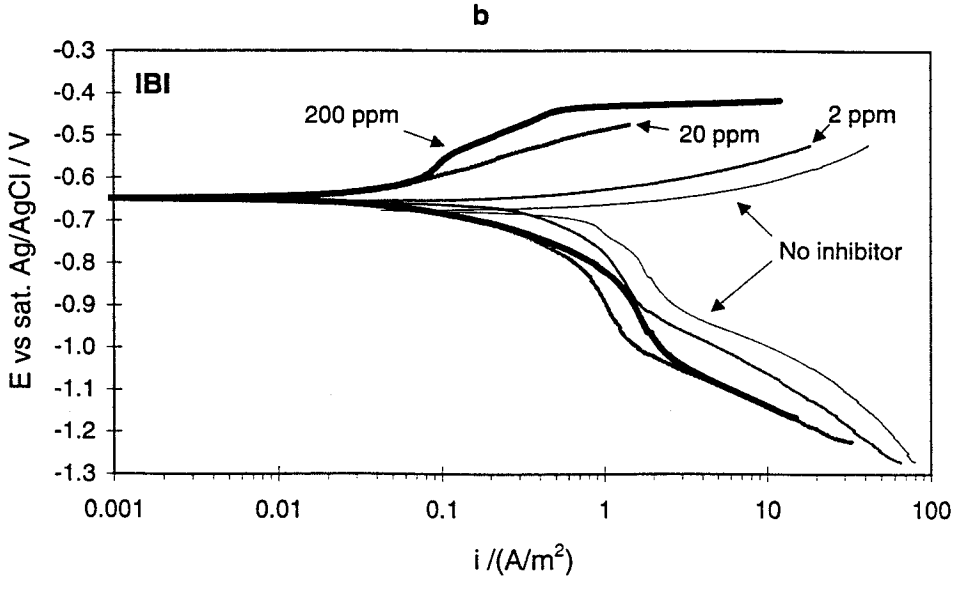

Figure 6. The effect of inhibitor concentration on the potentiodynamic sweeps; pH 4, t=20°C, pco_2=1 bar, stagnant; a) amine based inhibitor (ABI), b) imidazoline based inhibitor (IBI).

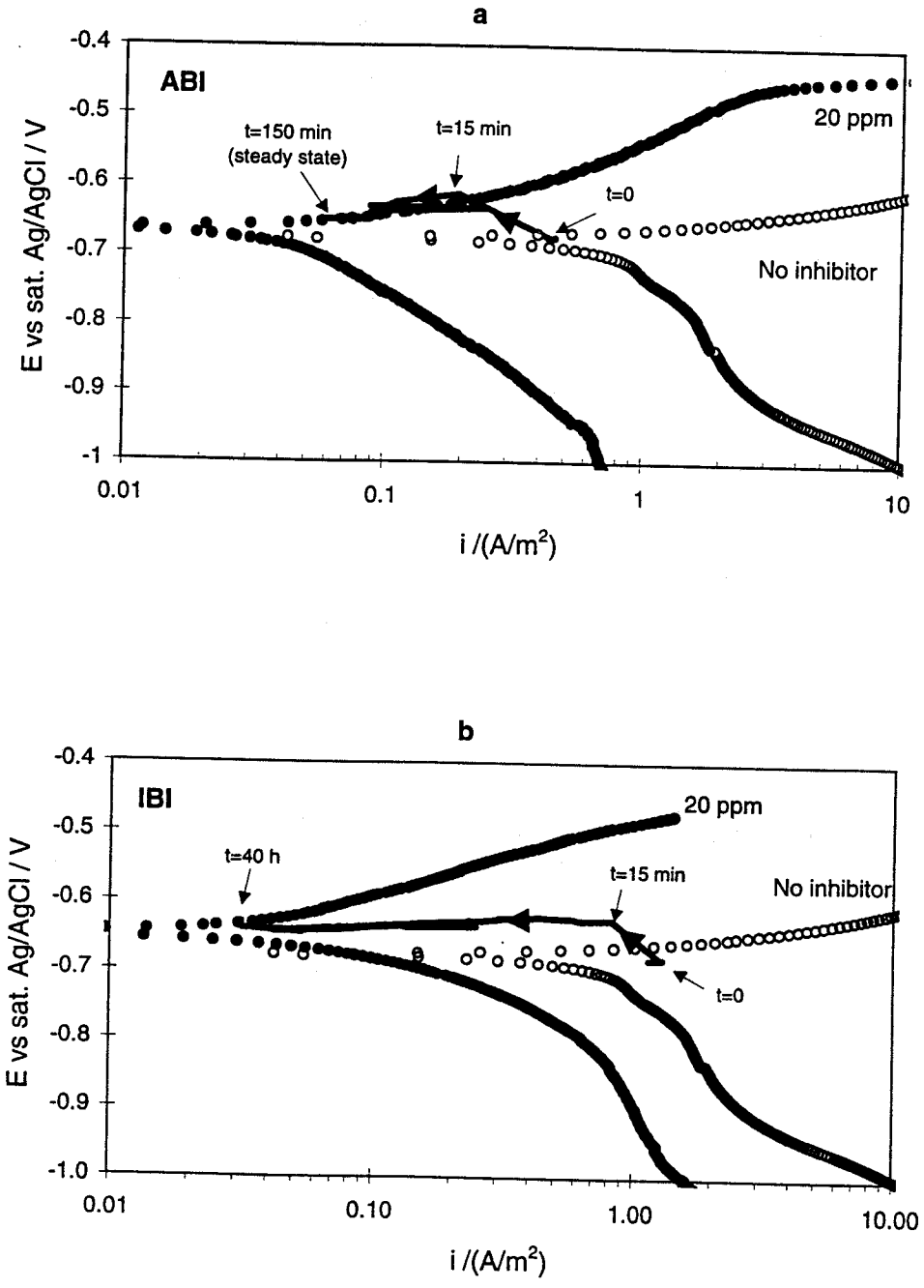

Figure 7. Trajectory of the "corrosion point" when 20 ppm of inhibitor was added at pH 4, t=20°C, p_{CO_2}=1 bar, stagnant; a) amine based inhibitor (ABI), b) imidazoline based inhibitor (IBI).

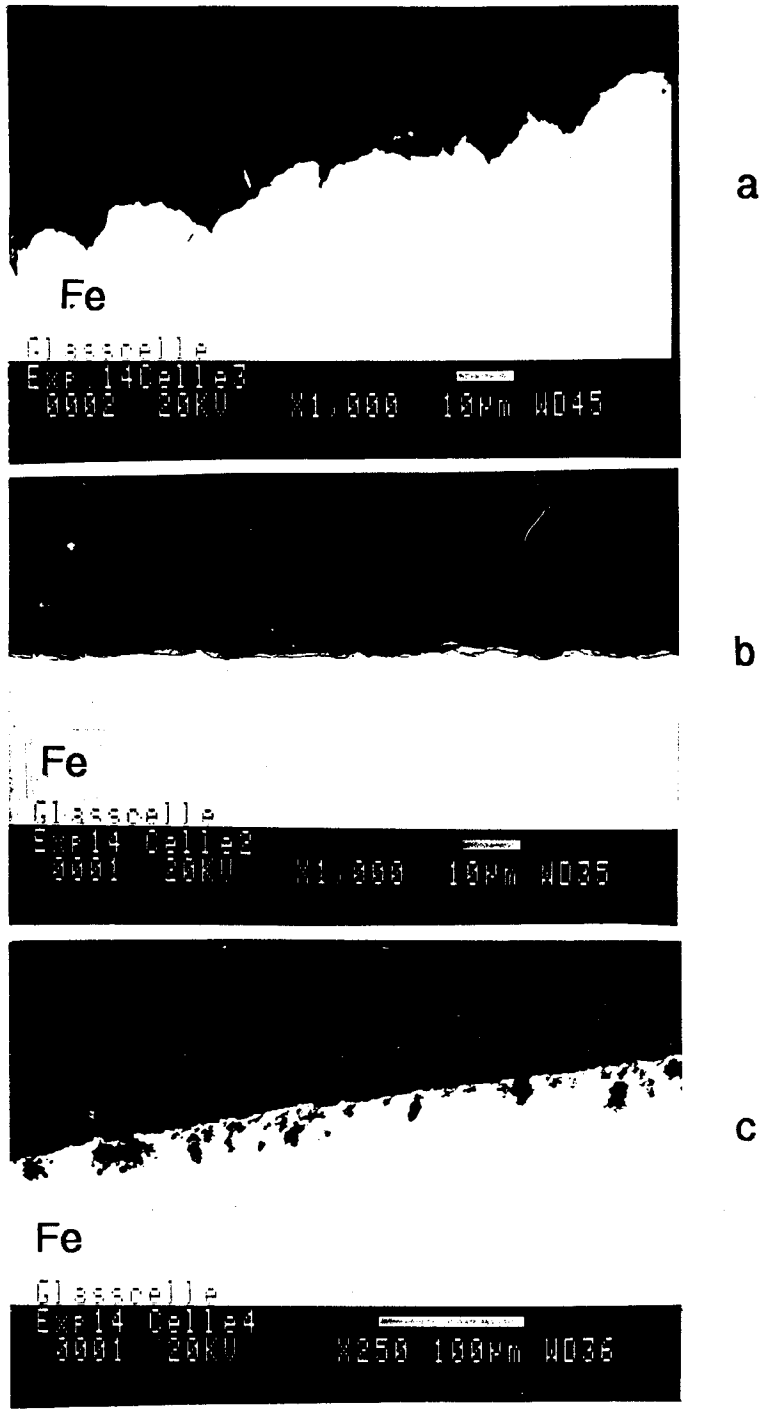

Figure 8. *SEM images of the cross section of the metal surface for (a) 2* ppm, *(b) 20* ppm, *(c) 200 ppm IBI concentration; pH 4, t=20°C, p_{CO_2}=1 bar, stagnant.*

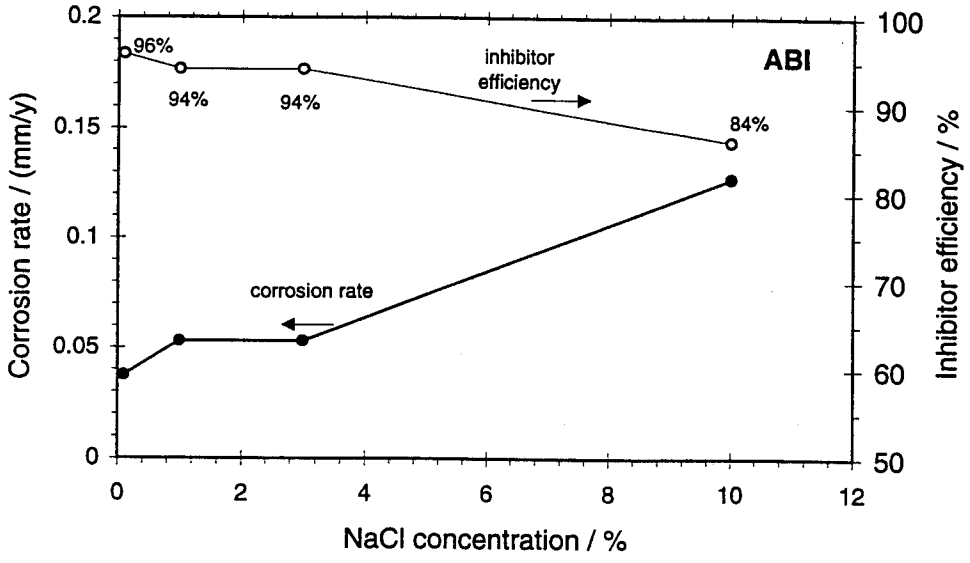

Figure 9. Effect of NaCl concentration on the performance of the amine based inhibitor; c_{inh}=20 ppm, pH 4, t=20°C, p_{CO_2}=1 bar, stagnant.

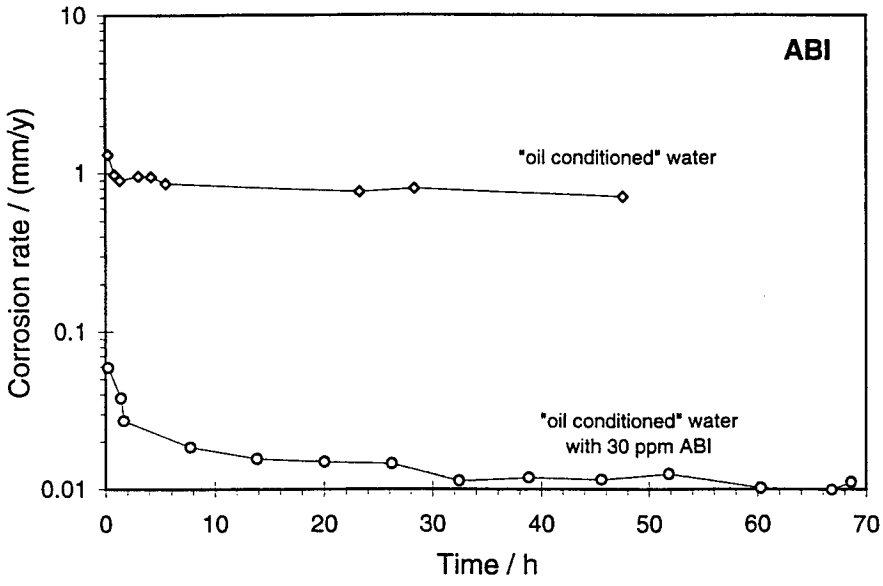

Figure 10. The effect of "oil-conditioning" and inhibitor partitioning on the performance of the amine based inhibitor (ABI) ; pH 4, t=22°C, pco_2=1 bar, stagnant.

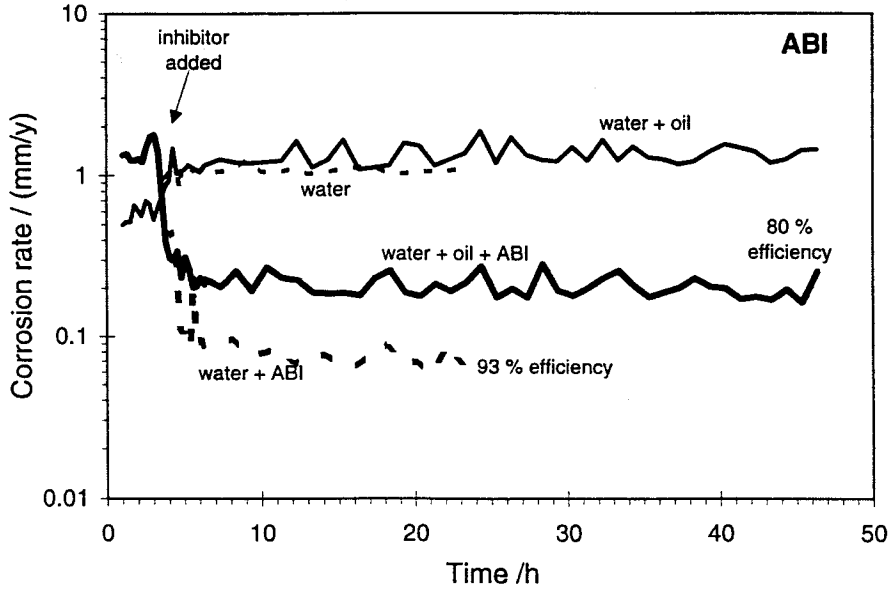

Figure 11. Effect of the crude oil on the performance of the amine based inhibitor; c_{inh}=20 ppm, pH 4, t=20°C, pco_2=1 bar, stagnant.

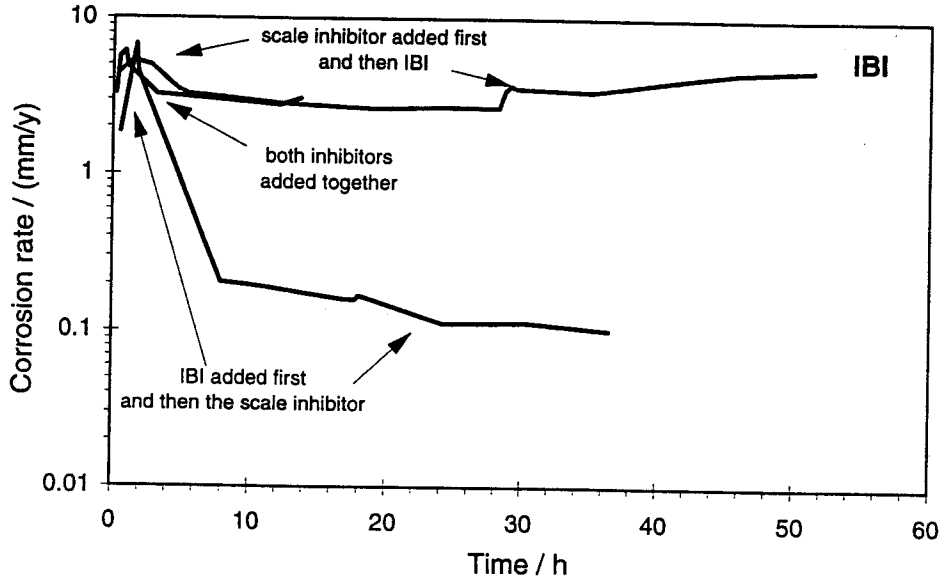

Figure 12. The compatibility of the imidazoline based corrosion inhibitor (30 ppm) with a phosphinocarboxylic acid based scale inhibitor (50 ppm); pH≥4, t=50°C, pco_2=2 bar, stagnant.

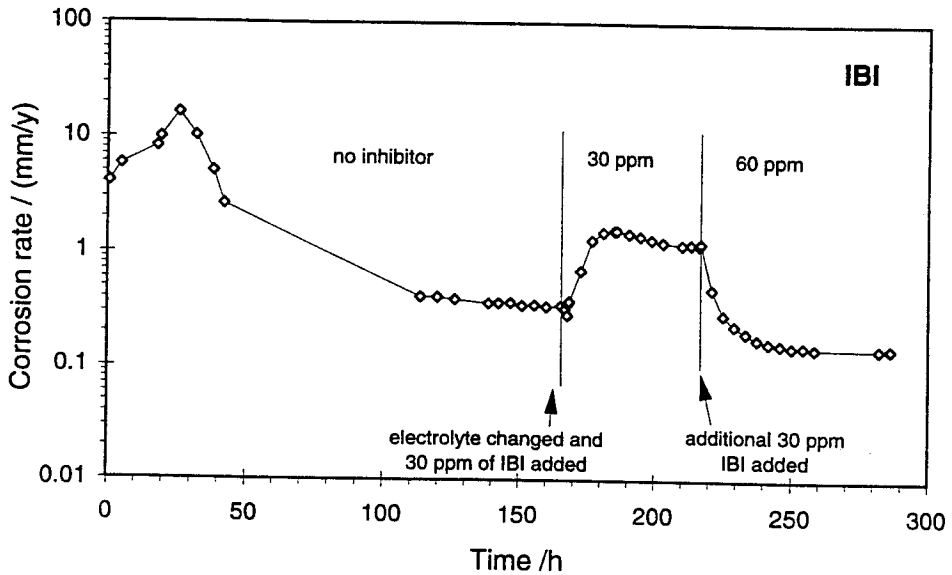

Figure 13. Effect of specimen precorrosion in the autoclave on the performance of the imidazoline based corrosion inhibitor (IBI) inhibitor; c_{inh}=30/60 ppm, pH≥4, t=80°C, pco_2=2 bar, stagnant.

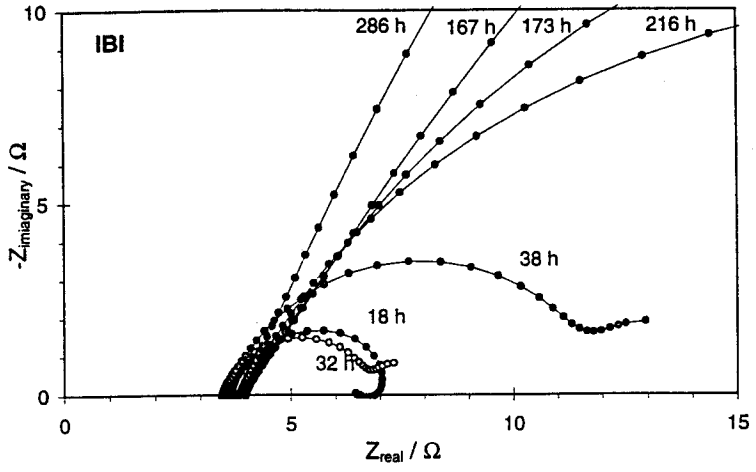

Figure 14. AC impedance measurements; conditions as in Figure 13.

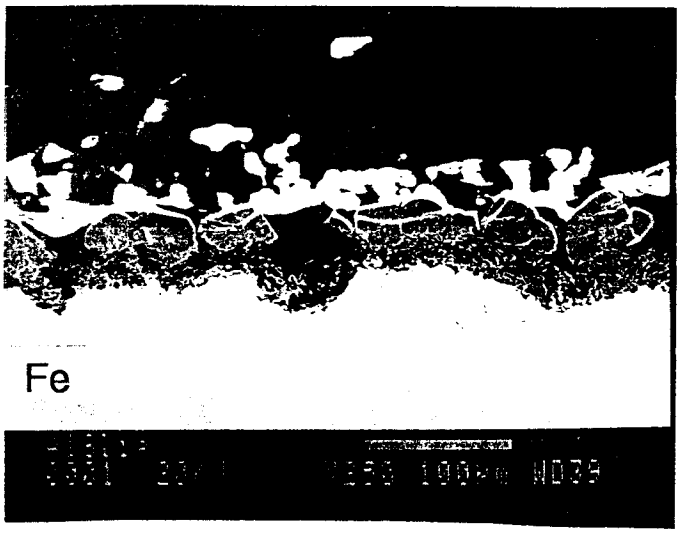

Figure 15. SEM image of the cross section of the specimen surface precorroded in the autoclave; conditions as in Figure 13.

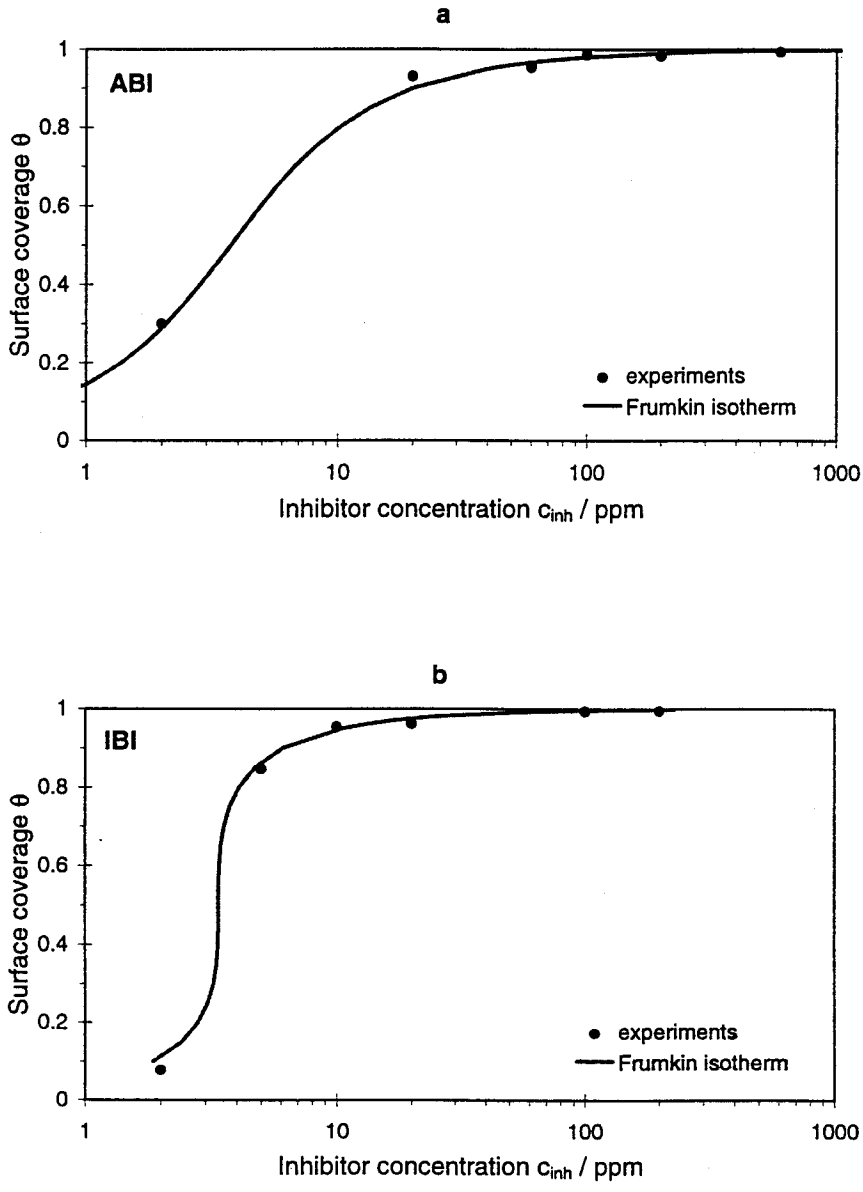

Figure 16. Calculated electrode surface coverage as a function of the inhibitor concentration; pH 4, t=20°C, pco_2=1 bar, stagnant a) amine based inhibitor (ABI), b) imidazoline based inhibitor (IBI).

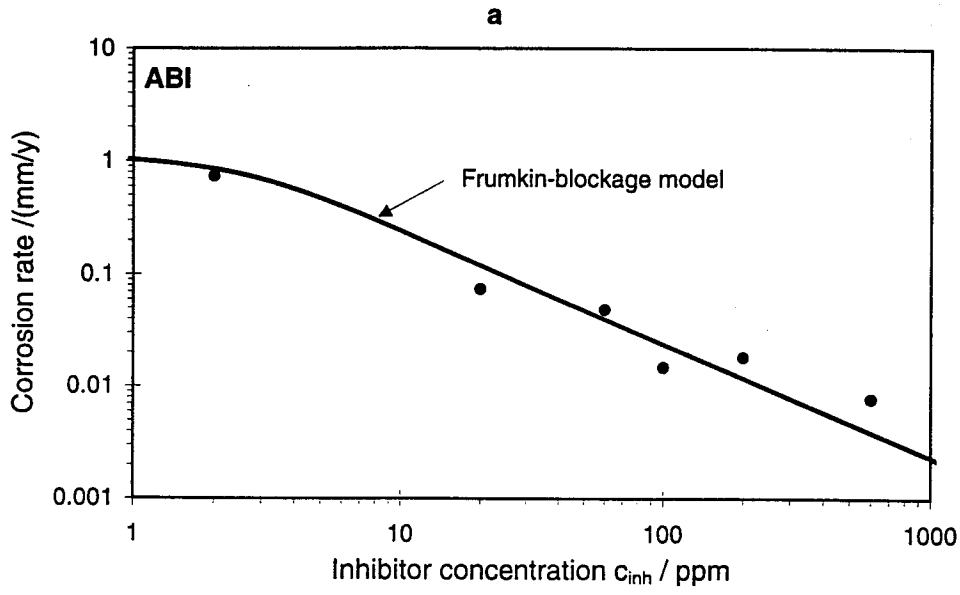

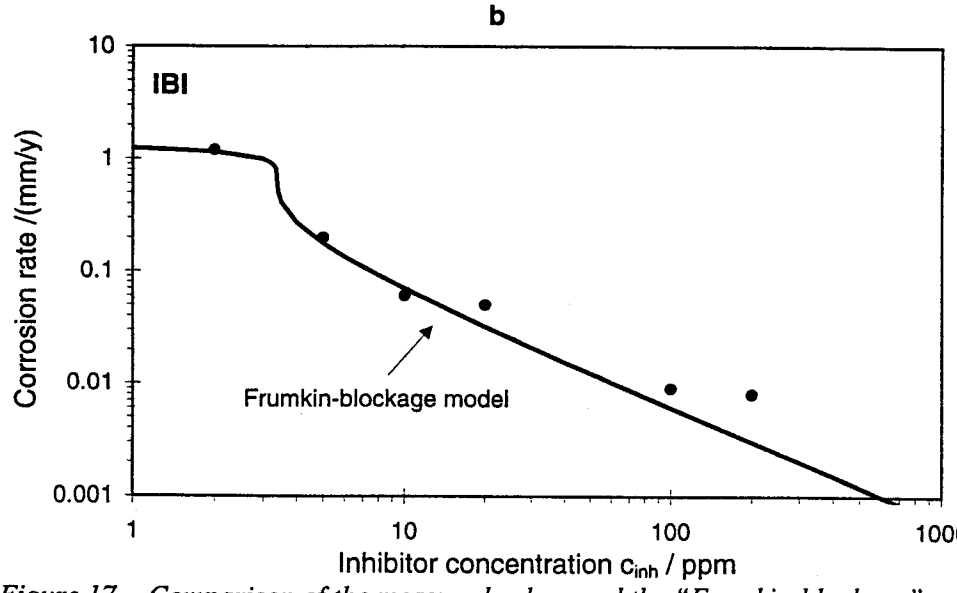

Figure 17. Comparison of the measured values and the "Frumkin-blockage" models for prediction of inhibitor performance at pH 4, t=20°C, p_{CO_2}=1 bar, stagnant; a) amine based inhibitor (ABI), b) imidazoline based inhibitor (IBI).